ELSEVIER

Journal of Nuclear Materials 283–287 (2000) 528–534

journal of nuclear materials

www.elsevier.nl/locate/jnucmat

Deformation mechanisms in 316 stainless steel irradiated at 60°C and 330°C

N. Hashimoto [a,*], S.J. Zinkle [a], A.F. Rowcliffe [a], J.P. Robertson [a], S. Jitsukawa [b]

[a] *Metals and Ceramics Division, Oak Ridge National Laboratory, Building 5500 MS 6376, P.O. Box 2008, Oak Ridge, TN 37831-6376, USA*

[b] *Japan Atomic Energy Research Institute, Tokai-mura Ibaraki-ken 319-1195, Japan*

Abstract

Plastically deformed microstructures in neutron-irradiated austenitic stainless steel were investigated by transmission electron microscopy (TEM). Neutron irradiation at 60°C and 330°C to about 7 dpa induced a high number density of faulted loops and black dots, which resulted in irradiation-induced hardening. In the specimen irradiated at 60°C and tensile tested at 25°C at a strain rate of 4×10^{-4} s^{-1}, the deformation microstructure consisted of twins, elongated faulted loops, and lath and twin martensite phase. In the specimens irradiated and tested at 330°C at a strain rate of 4×10^{-4} and 4×10^{-6} s^{-1}, in addition to these features, dislocation channeling was also observed. The TEM examination suggests that lath and twin martensite can form during tensile testing at both of these temperatures. Examination of the specimens irradiated and tensile tested at 330°C indicated that twinning was the predominant deformation mode at slower strain rate and dislocation channeling was favored at higher temperature. From the micrographs taken from the {1 1 1} plane streak in a diffraction pattern, it is suggested that faulted loops could be the principal twin initiation site during deformation.

PACS: 61.72

1. Introduction

An austenitic stainless steel was selected for the first wall and shielding structural material of the international thermonuclear experimental reactor (ITER) [1], because in addition to favorable strength, toughness, and fabrication properties, there is an enormous reservoir of experience in fabricating and operating code-qualified austenitic stainless steel components in nuclear systems. In austenitic stainless steel, however, a drastic loss of uniform elongation and work hardening capacity are often observed in tensile tests after irradiation at temperatures between 200°C and 350°C [2–4]. A general tendency has been established in many alloy systems that the defect microstructure evolution and increase in strength could influence intergranular cracking or irradiation-assisted stress corrosion cracking (IASCC) susceptibility, and the inhomogeneous deformation that often occurs in hardened microstructures could promote dislocation pileups and high local stresses. However, the understanding of radiation hardening effects on the deformation of neutron-irradiated stainless steels is limited, and it is therefore important to clarify the mechanisms of deformation in neutron-irradiated austenitic stainless steels. The current work uses transmission electron microscopy (TEM) to examine the microstructure in neutron-irradiated austenitic stainless steels and how it influences hardening and plastic deformation.

2. Experimental procedure

A J316 austenitic stainless steel in a solution annealed (SA) condition was irradiated to about 7 dpa in the Oak

* Corresponding author. Tel.: +1-865 576 2714; fax: +1-865 574 0641.

E-mail address: hashimoton@ornl.gov (N. Hashimoto).

0022-3115/00/$ - see front matter
PII: S0022-3115(00)00087-8

Table 1
Chemical composition of the J316 used in this experiment (wt%)

	Fe	Cr	Ni	Mo	Mn	Si	C	S	P
J316	Bal.	16.75	13.52	2.46	1.80	0.61	0.058	0.003	0.028

Ridge research reactor (ORR) in the dual-temperature capsules designated ORR-MFE-6J (which operated at 60°C) and ORR-MFE-7J (which operated at 330°C). The irradiation in the ORR produced approximately 75–100 appm He in the steel, giving a fusion-relevant He/dpa ratio of about 11 appm/dpa [5–7]. The irradiated tensile specimens were in the form of SS-1 flat tensile specimens with an overall length of 44.45 mm. The gage section of the specimen is 20.32 mm long by 1.52 mm wide by 0.76 mm thick. Using an Instron universal testing machine for the tensile testing, the specimens irradiated at 60°C were tested at room temperature (25°C) in air with a strain rate of 4×10^{-4} s^{-1} and the specimens irradiated at 330°C were tested at 330°C under vacuum with strain rate of 4×10^{-4} and 4×10^{-6} s^{-1}. The 0.2% offset yield strength (YS), ultimate tensile strength (UTS), uniform elongation (E_U), and total elongation (E_t) were calculated from the engineering load-elongation curves. Some of these tensile property data were already reported in a previous paper [2].

The chemical composition of the J316 used in this study is given in Table 1. The TEM specimens were taken from the deformed area of tensile specimens after testing. Electron microscopy observations were performed with the JEM-2000FX transmission electron microscope operating 200 kV at Oak Ridge National Laboratory.

3. Results

3.1. Tensile properties of J316 irradiated at 330°C and 60°C

Fig. 1 shows the engineering stress–strain curves for the specimens, which include some previous data for comparison. Irradiation at 60°C results in an approximately threefold increase in yield stress. Following an initial yield drop, the material exhibits a slight amount of work hardening and elongates ~20% before necking and failure occur. The material work hardens after the yield point but the UTS is less than 10% higher than the YS. After irradiation and testing at 330°C, the deformation behavior is significantly different. The increase in yield stress is greater than that at 60°C by ~200 MPa. Shortly after yielding, the material does not exhibit any work hardening capacity. The uniform elongation is less than 0.5% and failure occurs after only ~3% total elongation. The tensile data of the specimen tested at the slower strain rate shows approximately the same trend to that tested at the faster strain rate.

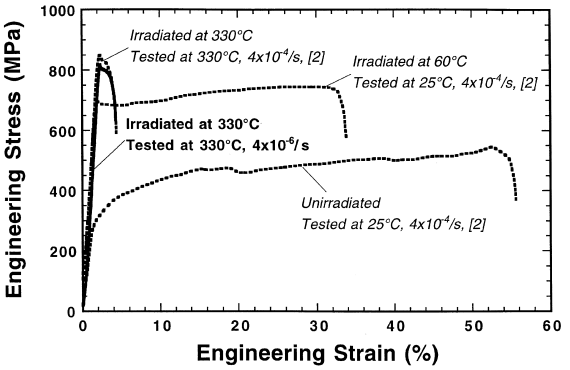

Fig. 1. The engineering stress–strain curve for the specimen irradiated and tested at 330°C with 4×10^{-6} s^{-1} strain rate. Some previous data are shown as a comparison.

3.2. Microstructure of tensile-tested J316 stainless steel after neutron irradiation

3.2.1. Microstructure of J316 irradiated and tensile-tested at 60°C

Fig. 2 shows faulted loops on {1 1 1} planes (Frank loops) and small defect clusters (black dots) in J316 stainless steel after irradiation at 60°C to 6.9 dpa and tensile testing at 25°C with a strain rate of 4×10^{-4} s^{-1}. The small defect clusters are probably dislocation loops and/or stacking fault tetrahedra (SFT) [8], but they are too small to determine their morphology or crystallography from the images. Figs. 3–5 show the deformation microstructures of J316 irradiated at 60°C and tensile tested at 25°C with a strain rate of 4×10^{-4} s^{-1}. Twins and extended stacking faults were observed in the matrix as shown in Fig. 3. Furthermore, lath and lens martensite structures, which were identified by diffraction pattern analysis, were found in the matrix as shown in Figs. 4 and 5. Twins and lens martensites were observed on {1 1 1} planes. Distinction between twins and lens martensites could be made by difference of distribution. The distribution of twins was homogeneous in the matrix, while lens martensites localized in bands or islands.

3.2.2. Microstructure of J316 irradiated and tensile-tested at 330°C

Fig. 6 shows the microstructure of J316 stainless steel tensile tested at 330°C with a strain rate of 4×10^{-4} s^{-1} after irradiation at 330°C to 7.4 dpa. The irradiation at 330°C induced a slightly higher Frank loop density

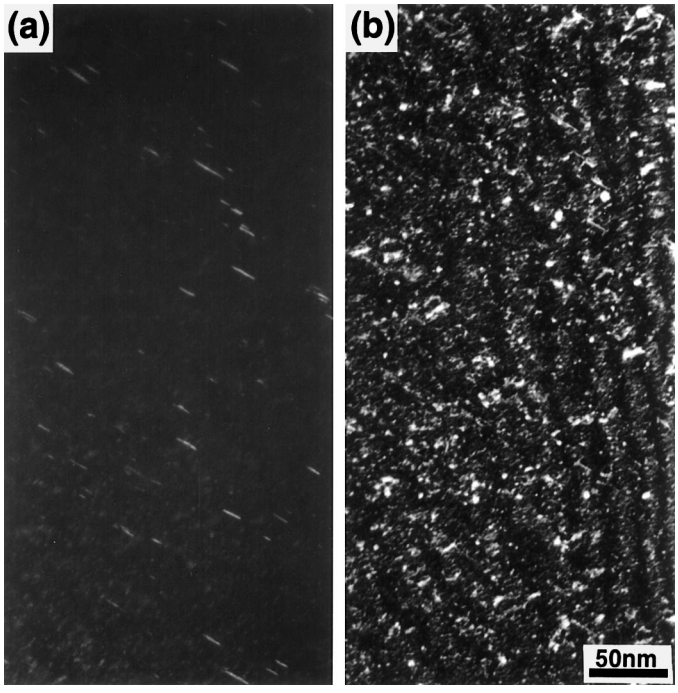

Fig. 2. Micrographs of (a) faulted loops on {1 1 1} plane (Frank loops) and (b) small defect clusters (black dots) in J316 stainless steel after irradiation at 60°C to 6.9 dpa. The micrographs were taken with beam direction B close to [0 1 1]. (a) is a dark-field image taken using streaks in the diffraction pattern arising from the faulted loops, and (b) is a weak-beam dark-field image, which was obtained on the diffraction conditions: $B \approx [0\,1\,1]$, $g = 200$, (g, $5g$).

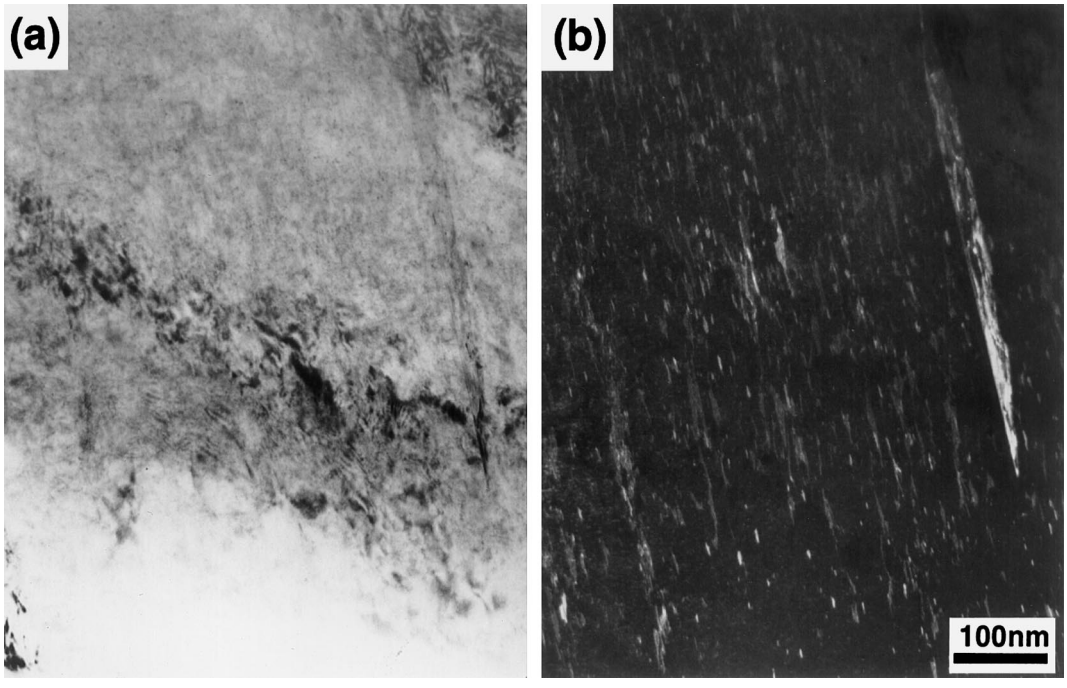

Fig. 3. Deformation twins and elongated loops in J316 irradiated at 60°C to 6.9 dpa and tensile tested at 25°C with faster strain rate of 4×10^{-4} s^{-1}. (a) is a bright-field image and (b) is a dark-field image taken using 111 streaks in the diffraction pattern.

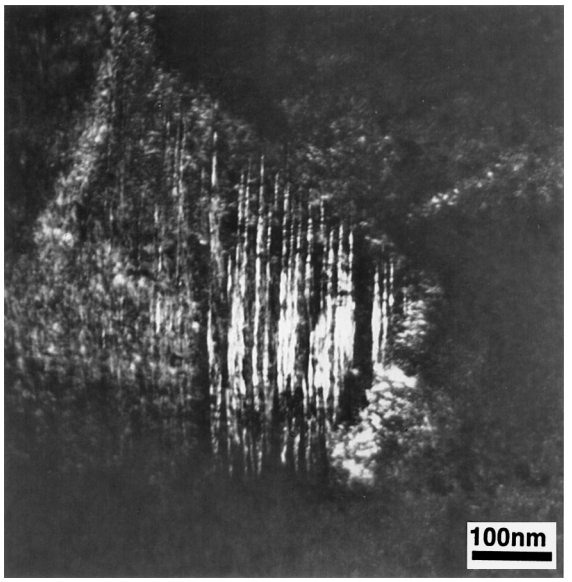

Fig. 4. Lens martensite in J316 irradiated at 60°C to 6.9 dpa and tensile tested at 25°C with faster strain rate of 4×10^{-4} s^{-1}. (a) is a bright-field image and (b) is a dark-field image taken using 1 1 1 streaks in the diffraction pattern.

compared with the irradiation at 60°C, while the number density of black dots in the specimen irradiated at 60°C is higher than that at 330°C. A summary of the defects observed in neutron-irradiated J316 is given in Table 2. In this irradiation and tensile testing condition, dislocation channels as indicated by cleared paths through the defect structure were also observed in the matrix as shown in Fig. 6. Twins, extended stacking faults and lath martensite structure were also found in the matrix.

In the specimen tensile tested at 330°C with the slower strain rate of 4×10^{-6} s^{-1} after irradiation at 330°C to 7.4 dpa, dislocation channels were observed in the matrix, similar to what was observed at 330°C for the faster strain rate. Lath and lens martensite were also found in this specimen, while twins were not observed compared with martensites.

4. Discussion

The ORR irradiation up to about 7 dpa induced faulted dislocation loops and resolvable but unidentifiable 'black dot' defect clusters. The faulted loops formed at 60°C and 330°C were identified as Frank type loops lying on {1 1 1} planes with Burgers vectors of type $\boldsymbol{b}=(1/3)\boldsymbol{a}_0\langle1\,1\,1\rangle$. The dislocation loop density at 330°C is higher than that at 60°C. Previous studies have shown that both the nature and number density of defects formed in type 316 austenitic stainless steel during neutron irradiation are strongly dependent on irradiation temperature [9–11]. Previous work [12,13] has characterized a low temperature regime as extending

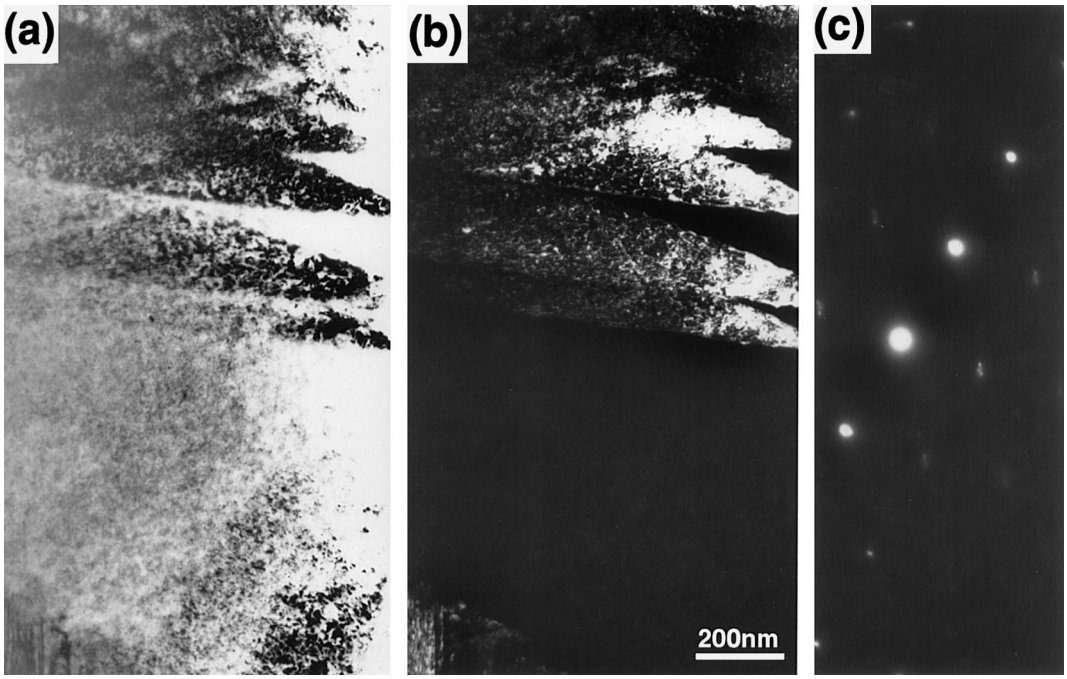

Fig. 5. Lath martensite in J316 irradiated at 60°C to 6.9 dpa and tensile tested at 25°C with faster strain rate of 4×10^{-4} s^{-1}.

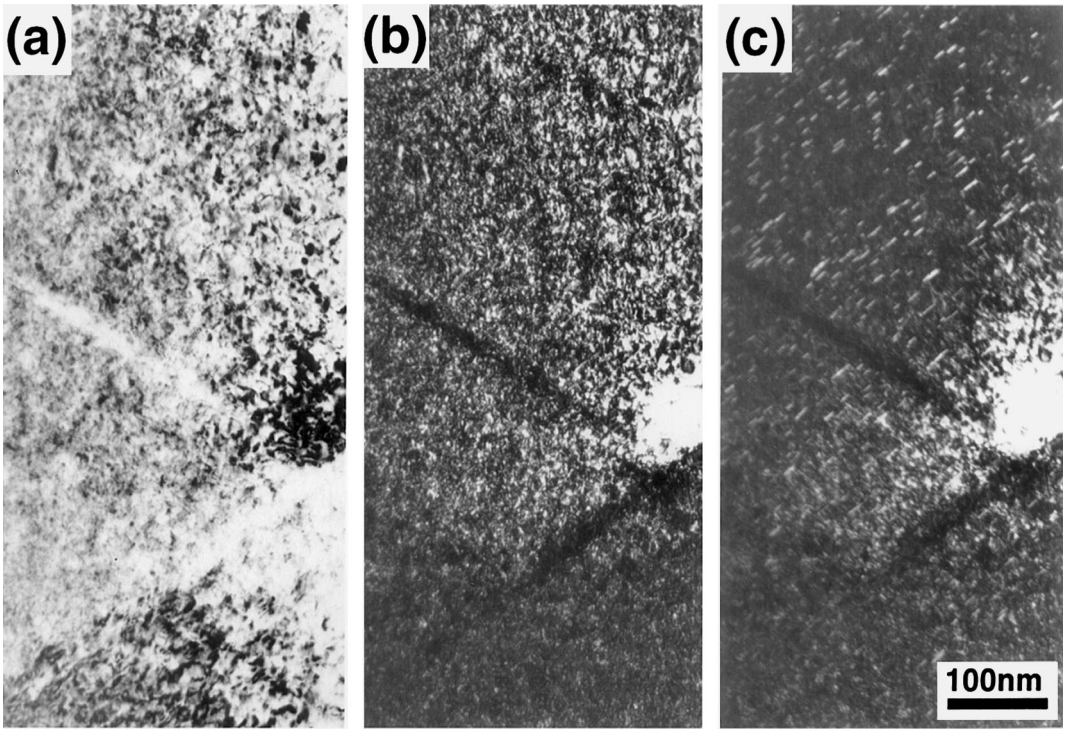

Fig. 6. Microstructure of J316 stainless steel tensile tested at 330°C with faster strain rate of 4×10^{-4} s^{-1} after irradiation at 330°C to 7.4 dpa. The electron micrographs were taken with beam direction B close to [0 1 1]. (a) is a bright-field image, (b) is a weak-beam dark-field image obtained on the diffraction conditions: $B\approx[0\,1\,1]$, $g=200$, (g, $5g$), and (c) is a dark-field image taken using 1 1 1 streaks in the diffraction pattern arising from the faulted loops. Dislocation channels are indicated by cleared paths through the defect structure were observed in matrix.

Table 2
Summary of defects in neutron-irradiated J316

Condition	Black dot		Faulted loop	
	Number density (m^{-3})	Mean size (nm)	Number density (m^{-3})	Mean size (nm)
Irradiation at 60°C	2.2×10^{23}	1.2	3.5×10^{22}	7.6
Irradiation at 330°C	1.1×10^{23}	1.2	5.5×10^{22}	8.0

from the onset of vacancy motion up to the temperature where vacancy clusters created in the displacement cascade become thermally unstable. The number densities of faulted Frank loops reported here are consistent with the values of previous reports for irradiation at low temperature [8,14,15].

The TEM examination of tensile tested J316 stainless steel shows not only radiation-induced defects but also stress-induced transformations. Twins were observed in the specimens tensile tested at the faster strain rate, but not at the slower strain rate at 330°C. According to a study of ion bombarded 304 stainless steel [16], deformation by twinning is the favored mode at faster strain rates and at lower temperatures. In the present experiment, however, twinning was observed in the specimens tensile tested not only at the lower temperature (60°C) but also at the higher temperature (330°C). The nature of the specific microstructural defect will determine its effectiveness in blocking dislocation motion and promoting radiation hardening. Frank loops formed during irradiation increase the stress required for dislocation slip above that for twin nucleation. Previous studies of plastic deformation of irradiated stainless steel [17,18] showed an increase of twinning at Frank loop sites. These microstructural variations can be assisted by the interaction of glide dislocations with Frank loops. Intersection of moving dislocations with a single Frank loop may occur in parallel glide planes of the same slip system, particularly with large faulted loops observed in low stacking fault energy (SFE) materials irradiated at

elevated temperatures. Once the partial dislocation dipoles break up with the assistance of thermal activation or local stress concentration, like partials will move in a common direction in accordance with the local shear stress, which could lead to the formation of a twin.

According to Song et al. [19], the partial perfect dislocation loops resulting from unfaulting of Frank loops are expected to be elongated during subsequent plastic deformation [19]. Elongated loops and dipoles have also been reported in irradiated Cu after tensile testing [20]. However, elongated loops could not be observed in this experiment. On the other hand, extended stacking faults on {1 1 1} planes were observed in the specimens tensile tested at 60°C and 330°C. The direction of the local shear stress near the Frank loops determines primarily whether unfaulting or stacking fault extension occurs in low stacking SFE materials, and unfaulting is more likely to occur than stacking fault extension because of the extra stress requirement for offsetting the SFE [19]. However, stacking fault extension is expected to occur after sufficient stress has been accumulated.

In the specimens irradiated and tensile tested at 330°C (which showed the loss of work hardening capacity), dislocation channels were observed in the matrix. In the channeling process, the movile dislocations cut, annihilate, and/or combine with the defects on the slip plane during glide. Subsequent dislocations will tend to glide along this same path, clearing out additional defects resulting in a channel free of defects. The increased slip band spacing that results from dislocation channeling reduces macroscopic displacement over a fixed dimension and hence reduces bulk ductility. Such channels have been seen in a wide variety of materials [21,22]. In this experiment, neutron-irradiation at the higher temperature induced a quite high density of Frank loops in the matrix, resulting in severe reduction of work hardening capacity and a decrease in uniform elongation. Additional loss of work hardening capacity was associated with dislocation channeling. It was previously reported that dislocation channeling in irradiated stainless steel is favored at higher temperature and at slower strain rates [16]. In the present experiment, dislocation channels were observed in the specimens at 330°C at both fast and slow strain rate. These observations would suggest that dislocation channeling is much more detrimental to ductility than mechanical twinning and martensite formation at the higher temperature for strain rates up to at least 4×10^{-4} s^{-1}. The effect of very high strain rates (e.g. >0.1 s^{-1}) on dislocation channeling still needs to be investigated.

As mentioned in section 3.2, The TEM examination showed the transformation of lath and lens martensite phases occurred in neutron-irradiated J316 stainless steel during deformation. Loss of work hardening and hence uniform elongation is generally attributed to the nature of the interactions between dislocations and the irradiated microstructure. Dislocation interaction with obstacles in unirradiated material leads to dislocation multiplication and, in some austenitics, to plasticity-induced martensite formation [23]; both of these lead to substantial work hardening of the material. Bressanelli and Moskowitz [24] studied the effects of composition, test temperature, and deformation rate on the tensile properties of type 301 stainless steel and clearly demonstrated the beneficial effect of a specific amount of martensite formation on tensile elongation. Tensile tested Fe–19%Cr–11%Ni austenitic stainless steel showed the deformation-induced martensite formation between the M_s and M_d temperatures (M_s: −70°C, M_d: 130°C) [25]. In general, the formation of martensite can be induced by elastic [26,27] and/or plastic [28–31] deformation between the M_s and M_d temperatures. At temperatures near M_s the stress required for slip in the austenitic matrix exceeds that necessary for the martensitic transformation. Conversely, as the temperature increases toward the M_d temperature, the stress required for martensite formation increases to a level above that required for slip in the austenite. Since the martensite transformation is a diffusionless shear transformation aided by positive normal stresses [26,27], basically it can be made to occur during deformation of the austenite at temperatures above M_s, while no deformation-induced transformation is possible above a certain temperature, M_d. In neutron-irradiated J316 stainless steel, however, deformation-induced transformation of martensite occurred not only at lower temperature (25°C) but also at higher temperature (330°C). Neutron irradiation induced a high density of faulted loops (Frank loops) and black dots (dislocation loops or SFTs). As mentioned above, it could be possible for planar defects to be nucleation sites of twins during deformation. According to previous papers [28,31], strain induced stacking faults may be the nucleation sites of the martensite. Therefore, it would suggest that the irradiation-induced planar defects (Frank loops) could play a role in the formation of martensite via nucleation of twins. Furthermore, small amounts of plastic deformation tend to promote the formation of martensite in ferrous alloys with a low stacking fault energy [32].

5. Conclusions

Tensile-tested specimens of an annealed austenitic stainless steel J316 irradiated at 60°C and 330°C have been investigated by transmission electron microscopy. The irradiations introduced Frank loops and black dots in the matrix. The TEM examination of tensile tested J316 stainless steel shows not only radiation-induced defect formation but also twinning, stacking fault ex-

tension, dislocation channeling, and deformation-induced martensite transformation.

1. A strong temperature dependence of twinning was not observed in this experiment, although there was a tendency for reduced twinning at lower temperatures at higher strain rates. From the analysis of microstructure, it would suggest that Frank loops could be the principal twin sources.
2. Dislocation channels were observed only in the specimens which showed the most dramatic loss of work hardening capacity (330°C irradiation). Dislocation channeling could be the dominant deformation mechanism at the higher temperature. An effect of strain rate on dislocation channeling could not be detected in this experiment.
3. TEM examination showed the deformation-induced transformation of martensite occurred in neutron-irradiated J316 stainless steel. It is suggested that radiation-induced planar defects may be nucleation sites for twins during deformation and strain induced stacking faults may be the nucleation sites of the martensite.

Acknowledgements

The authors are grateful to Dr M.L. Grossbeck for providing valuable irradiated samples. They also would like to thank Y. Miwa for his helpful discussions, and grateful to Messrs. J.W. Jones, R.G. Sitterson, A.T. Fisher, and J.J. Duff for technical support. Particular thanks go to Mr L.T. Gibson for solving the difficult problems associated with the preparation of TEM specimens from the gage section of the irradiated tensile specimens. This research was supported in part by an appointment to the Oak Ridge National Laboratory Postdoctoral Research Associates Program administered jointly by the Oak Ridge Institute for Science and Education and Oak Ridge National Laboratory.

References

[1] A.F. Rowcliffe, ITER Material Assessment Report for Stainless Steels, ITER Doc. G A1 DDD 1 97-12-08 W 0.2, December, 1997.
[2] J.E. Pawel, A.F. Rowcliffe, D.J. Alexander, M.L. Grossbeck, K. Shiba, J. Nucl. Mater. 233–237 (1996) 202.
[3] G.E. Lucas, J. Nucl. Mater. 206 (1993) 287.
[4] D.J. Alexander, J.E. Pawel, M.L. Grossbeck, A.F. Rowcliffe, K. Shiba, Fusion Reactor Materials Semiannual Report, DOE/ER-0313/19, 1996, p. 204.
[5] I.I. Siman-Tov, Fusion Reactor Materials Semiannual Report, DOE/ER-0313/3, 1988, p. 7.
[6] L.R. Greenwood, Fusion Reactor Materials Semiannual Report, DOE/ER-0313/6, 1989, p. 23.
[7] L.R. Greenwood, D.V. Steidl, Fusion Reactor Materials Semiannual Report, DOE/ER-0313/8, 1990, p. 34.
[8] M. Horiki, M. Kiritani, J. Nucl. Mater. 212–215 (1994) 246.
[9] S.J. Zinkle, P.J. Maziasz, R.E. Stoller, J. Nucl. Mater. 206 (1993) 266.
[10] M. Kiritani, Ultramicroscopy 39 (1991) 135.
[11] P.J. Maziasz, C.J. McHargue, Int. Mater. Rev. 32 (1992) 190.
[12] J.W. Corbett, Electron Radiation Damage in Semiconductors and Metals, Solid State Physics, suppl. 7, Academic Press, New York, 1966.
[13] W. Schilling, P. Ehrhart, K. Sonnenberg, Fundamental aspects of radiation damage in metals, in: M.T. Robinson, F.W. Young Jr. (Eds.), vol. 1, CONF-751006-P1, NTIS, Springfield, VA, 1975, p. 470.
[14] P.J. Maziasz, J. Nucl. Mater. 205 (1993) 118.
[15] M.P. Tanaka, P.J. Maziasz, A. Hishinuma, S. Hamada, J. Nucl. Mater. 141–143 (1986) 943.
[16] S.M. Bruemmer, J.I. Cole, R.D. Carter, G.S. Was, Mater. Res. Soc. Symp. Proc. 439 (1997) 437.
[17] J.I. Cole, S.M. Bruemmer, J. Nucl. Mater. 225 (1995) 53.
[18] J.L. Brimhall, J.I. Cole, S.M. Bruemmer, Scripta Metall. Mater. 30 (1994) 1473.
[19] S.G. Song, J.I. Cole, S.M. Bruemmer, Acta Mater. 45 (1997) 501.
[20] J.V. Sharp, Philos. Mag. 16 (1967) 77.
[21] M.S. Wechsler, in: R.E. Reed-Hill (Ed.), The Inhomogeneity of Plastic Deformation, ASM, 1973, p. 19 (Chapter 2).
[22] A. Luft, Prog. Mater. Sci. 35 (1991) 97.
[23] D. Fahr, Metall. Trans. 2 (1971) 1883.
[24] J.P. Bressanelli, A. Moskowitz, ASM Trans. Quart. 59 (1966) 223.
[25] I. Tamura et al., in: Proceedings of the second International Conference on Strength of Metal and Alloys, ASM, 1970, p. 900.
[26] S.A. Kulin, M. Cohen, B.L. Averbach, Trans. AIME 194 (1952) 661.
[27] J.R. Patel, M. Cohen, Acta. Metall. 1 (1953) 531.
[28] B. Cina, Acta. Metall. 6 (1958) 748.
[29] J.A. Venables, Philos. Mag. 7 (1962) 35.
[30] J.F. Breedis, W.D. Robertson, Acta. Metall. 11 (1963) 547.
[31] R. Lagneborn, Acta. Metall. 12 (1964) 823.
[32] H.M. Otte, Acta. Metall. 5 (1957) 614.